Nanotechnology Perceptions
ISSN 1660-6795
www.nano-ntp.com

Impact of Different Mixing Techniques on Iron Oxide Nanoparticles Synthesized Via Co-Precipitation Method

Sunil M Badgujar[1,2], Ujwal D Patil[2], Jitendra S Narkhede[2]

[1]Department of Chemical Engineering, Shroff S.R. Rotary Institute of Chemical Technology, UPL University of Sustainable Technology, Ankleshwar, Gujarat-393001, India
[2]University Institute of Chemical Technology, KBC North Maharashtra University, Jalgaon Maharashtra-425001, India
Email: sunilmbadgujar@gmail.com

This research explores how different mixing methods impact the properties of iron oxide nanoparticles produced through the co-precipitation method. We conducted batch experiments using various mixing techniques, such as an ultrasonic bath and an overhead stirrer, to mix the reactants in the early stages. The iron oxide nanoparticles synthesized were analyzed using XRD, FESEM, EDX, and FTIR. From the XRD analysis, we determined the average crystal size of the nanoparticles under different mixing conditions. The crystal sizes observed were 33.60 nm without stirring, 26.54 nm with a stirring speed of 500 rpm, and 23.72 nm with an ultrasonication frequency of 40 kHz.

Keywords: Co-precipitation, Ultrasonication, Stirring, Nucleation.

Graphical Abstract

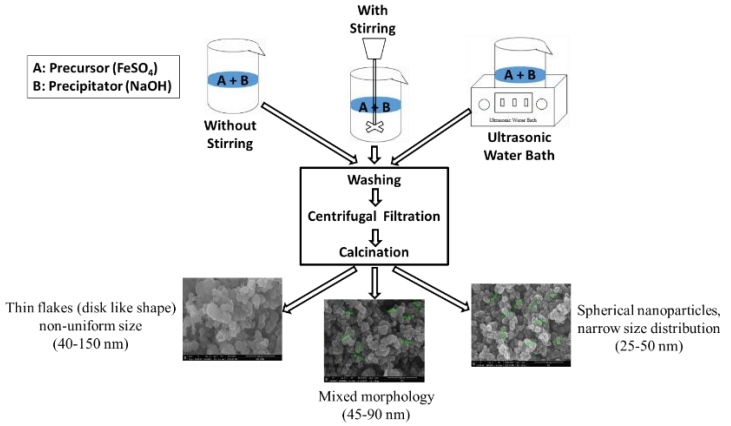

1. Introduction

Nanoscience and technology have become increasingly important due to the creation of a variety of functional materials that exhibit unique properties and enhanced performance, largely thanks to a higher surface-to-volume ratio. As particle size decreases, the proportion of surface atoms increases.[1]. The three most prevalent forms of iron oxides that are present in nature are magnetite (Fe3O4), maghemite (γ-Fe2O3), and hematite (α-Fe2O3). These iron oxides are not only prevalent in the natural world but also play a crucial role in scientific and technological research.[2]. Their versatile applications span numerous fields, including their use as catalysts, adsorbents, pigments, and coatings. They are also essential in printing inks, wastewater treatment, ion exchange, gas sensing, magnetic recording and data storage, bio-separation, drug delivery, and magnetic resonance imaging, among many other areas.[3]. Various physical, chemical, and biological methods have been adopted to synthesize iron oxide nanoparticle[4]. Amongst several methods of synthesis co-precipitation is the one of the most convenient method for iron oxide nanoparticle synthesis due to simple steps involved, reproducibility, cost involved[5]. The co-precipitation method involves several processes happening simultaneously, including nucleation, growth, coarsening, and agglomeration. Nucleation is a critical process that results in the formation of a significant number of microscopic particles. Other methodologies like Ostwald ripening and aggregation drastically influence the size, shape, and characteristics of the final products.[6]. The properties of co-precipitation product mainly depends on concentration of the reactants, temperature, pH, stirring speed, nature of the reactants etc.[7]. Studies have indicated that the complex processes underlying particle generation make it challenging to regulate iron oxide nanoparticle size. Notably, the most magnetic phase of iron oxide emerges within just 5 seconds after combining the ferrous/ferric chloride precursor with the NaOH base solution.[8]. The effect of stirring speed is greater on mass transfer than oxygen concentration in the solution[9]. The size of product particles is influenced by mixing, as evidenced by other research results. By increasing the agitation rate, smaller particles can be synthesised. [10]. In ultrasonication, depending on the sonication frequency the generated sound waves propagate into the liquid medium causing high pressure and low pressure regions. Formation of tiny bubbles occurs during the low pressure high intensity cycle and they collapse during the high pressure cycle[11]. The large magnitude of energy will be released due to the violent collapse of the cavities in ultrasonic bath reactor[12]. The research carried out to synthesis gold nanoparticles using conventional bath ultrasonication shows that the sonication has a significant effect on the particle size and morphology of gold nanoparticles[13]. The particle can grow by aggregation with each other until the critical size and growth of particles larger than critical size can be controlled by sonication. This effect reduces the number of large particles in the solution and reduces the particle size distribution[14]. The ultrasonic-assisted co-precipitation approach produced samples with more homogenous, smaller, and dispersed particles. This synergistic effect of the ultrasounds observed further support the co-precipitation synthesis, where ultrasound provides a favourable atmosphere for nucleation and development of the particles avoiding their aggregation. Higher irradiation power results into smaller size, more uniform nanoparticles and stronger interaction between metal oxides.[15]. The stoichiometric requirements of the reactants was decided form the reaction mechanism for iron oxide nanoparticle formation via co-precipitation using ferrous sulphate as precursors proposed by[16] is represented below:

$$Fe^{2+} + 2OH^{-} \rightarrow Fe(OH)_2$$

$$4Fe(OH)_2 + O_2 \rightarrow 4FeOOH + 2H_2O$$

$$Fe(OH)_2 + 2FeOOH \rightarrow Fe_3O_4 + 2H_2O$$

The present study focuses on the effect of stirring and ultrasonication on aggregation of particles during nucleation and growth steps. Overhead stirrer and bath sonication was used for synthesis of iron oxide by co-precipitation method.

2. Experiment

2.1 Materials

The analytical grade ferrous sulphate ($FeSO_4.7H_2O$), from s. d. Fine Chemicals and sodium hydroxide (NaOH) from Qualigens were used as received and the solutions were prepared in distilled water.

2.2 Method

The co-precipitation synthesis was performed at room temperature (30°C). As illustrated in Figure 1, 100ml of a 0.1M ferrous sulphate solution (A) and 100ml of a 0.2M sodium hydroxide solution (B) were quickly mixed in a beaker to synthesize iron oxide nanoparticles. The reaction was allowed to proceed for 30 minutes to enable nucleation and growth. The mixture was then left to age for 2 hours. After ageing, the precipitate was separated and washed 4-5 times with distilled water. The washing process was carried out using a Remi C-30 BL refrigerated centrifuge at 5000 rpm, -8°C, for 15 minutes. This washing was repeated until all unreacted NaOH and soluble impurities were removed. The resulting wet cake was dried at 200°C for 6 hours in an oven. The synthesis of iron oxide nanoparticles was conducted under various mixing conditions.

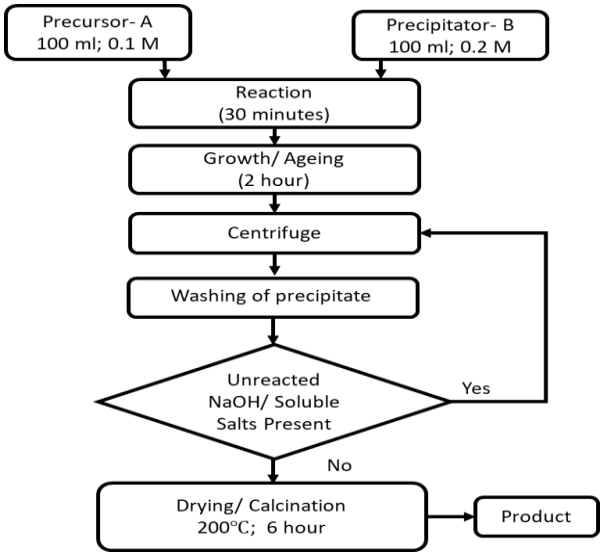

Fig. 1. Synthesis procedure for iron oxide nanoparticles.

2.2.1. Procedure 1 (Bulk addition without stirring/ sonication).

Figure 2 illustrates the steps involved in synthesizing iron oxide nanoparticles using Procedure 1. The reactants, (A) and (B), were added without stirring or ultrasonication into a 500ml glass beaker. The beaker was then placed in a water bath for 30 minutes to maintain isothermal conditions.

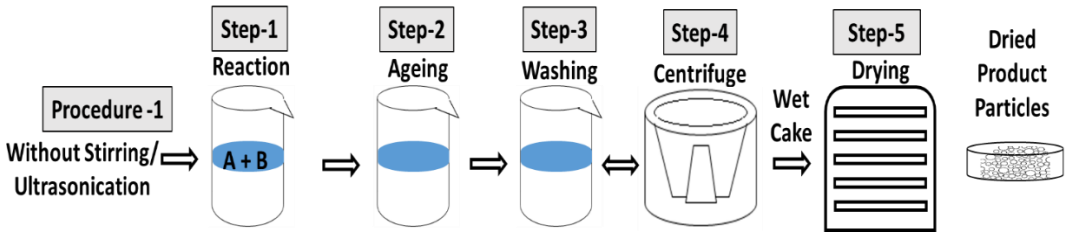

Fig. 2. Steps for synthesizing iron oxide nanoparticles using Procedure 1.

2.2.2. Procedure 2 (Reaction with stirring).

In procedure 2 the reactant (A) and (B) were mixed instantaneously in a 500ml glass beaker. The contents were agitated using overhead stirrer for 30 min at stirring speed of 500rpm. The isothermal conditions were maintained by keeping the beaker in water bath. Fig.3 represent the steps involved in the procedure-2.

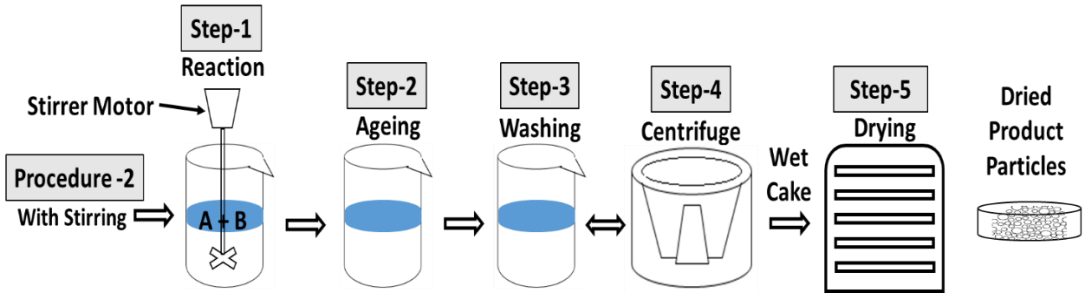

Fig. 3. Steps for synthesizing iron oxide nanoparticles using Procedure 2.

2.2.3. Procedure 3 (Reaction in bath sonicator).

In procedure 3 the reactant (A) and (B) were mixed instantaneously in a 500ml glass beaker kept in an ultrasonic water bath for 30 min. The isothermal conditions were maintained in ultrasonic water bath by continuous circulation of water. The bath has fixed ultrasound frequency of 40 kHz.

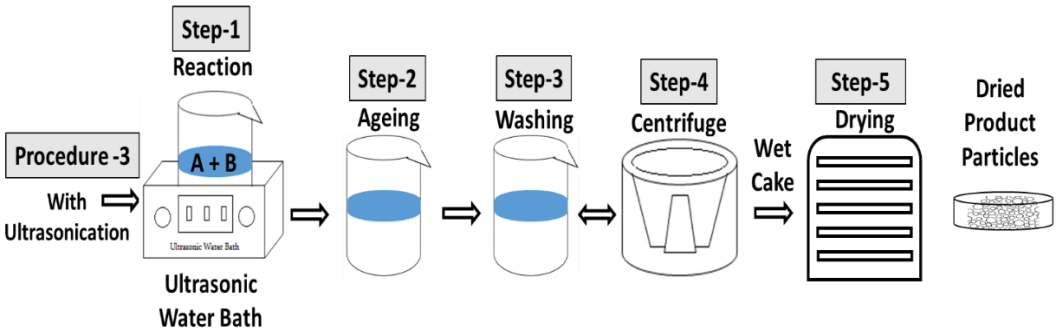

Fig. 4. Steps for synthesizing iron oxide nanoparticles using Procedure 3.

3. Result & Discussion

The iron oxide powder samples were characterized using XRD, FESEM, EDX and FTIR analysis. The results obtained are as shown below:

3.1. XRD analysis

The presence and size of the synthesised iron oxide nanoparticles were investigated through X-ray diffraction (XRD) analysis. For this analysis, a Bruker AXS GmbH D8 Advance X-ray diffractometer was used, which is equipped with a copper K-alpha (CuKα) radiation source. The measurements were performed over a 2θ range of 5 to 80 degrees. The purpose of using XRD is to identify the crystalline phases present in the nanoparticles and to estimate their average crystallite size. This is achieved by analyzing the diffraction patterns, which provide information about the crystal structure and lattice parameters. The characteristic peaks in the XRD pattern correspond to specific planes within the crystal structure, allowing for phase identification. By applying the Scherrer equation to the XRD data, the average crystallite size of the iron oxide nanoparticles can be calculated. This equation relates the broadening of the diffraction peaks to the size of the crystallites, providing an estimate of their average diameter. This analysis is crucial for understanding the structural properties of the nanoparticles. The average particle size of the synthesized iron oxide nanoparticles was determined using Scherrer's equation.

$$d = \frac{K\lambda}{\beta\cos\theta}$$

Where K is the Scherrer's constant (K=0.89), β is the full width of the peak at half maximum of the highest peak in the diffraction pattern obtained from XRD analysis, λ is the X-ray wavelength ($\lambda = 0.15406$ nm) and θ is the Bragg's diffraction angle. The average particle size obtained from XRD analysis different set of experiment is listed in Table 1:

Table 1: The average particle size obtained from XRD analysis

Sample Description	2θ Values in [°]	θ[°]	FWHM (β) [rad]	Size of particle in [nm]
Procedure-1	35.6127	17.80635	0.004189	33.60

Procedure-2	35.633	17.8165	0.005304	26.5433
Procedure-3	35.63	17.815	0.005934	23.72

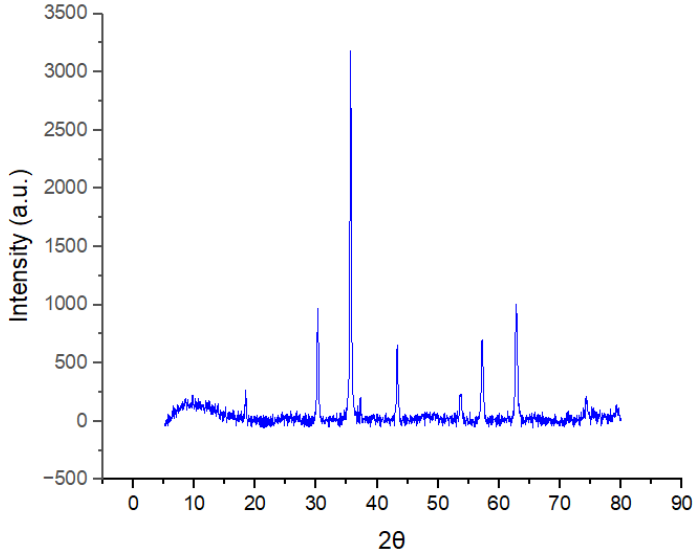

Fig. 5. X-Ray diffraction patterns of iron oxide synthesized without stirring or ultrasonication.

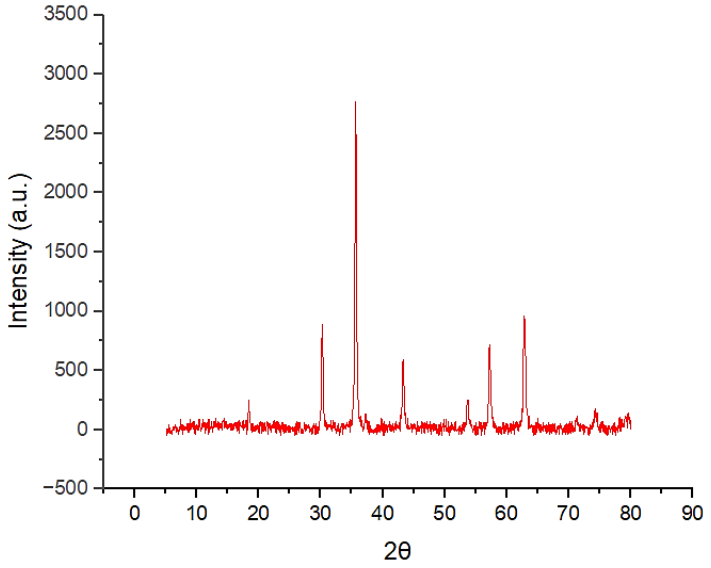

Fig. 6. X-Ray diffraction patterns of iron oxide synthesized with stirring speed.

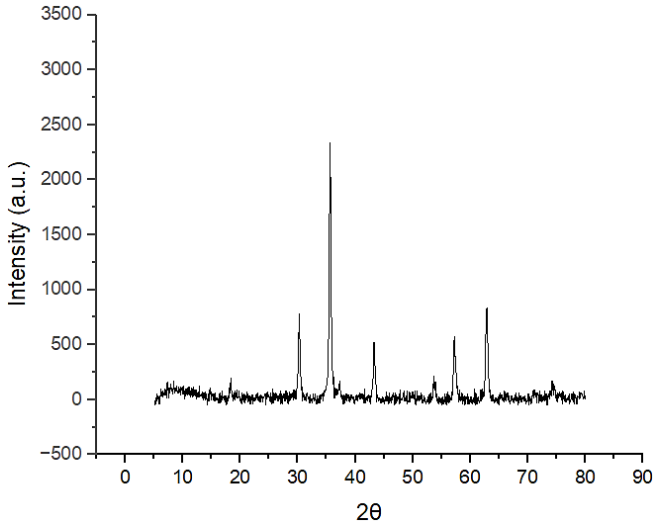

Fig. 7. X-Ray diffraction patterns of iron oxide synthesized using a bath sonicator.

The XRD diffraction patterns in Figures 5, 6, and 7 align with the standard reference peaks for magnetite (ICDD-19-629) and maghemite (ICDD-39-1346) iron oxide crystals. Although magnetite and maghemite have similar diffraction patterns, peaks were observed at 30.26°, 35.65°, 43.31°, 53.76°, 57.25°, and 62.80°. The dark brown colour of the product particles indicates the presence of maghemite. Sharp peaks in the XRD analysis suggest a crystalline nature, with a higher number of atoms or larger crystal sizes, while broader peaks indicate an amorphous nature. The peak intensity at 35.65° decreases for particles synthesized by Procedure-1, Procedure-2, and Procedure-3, respectively.

FESEM analysis

Figure 8 presents the Field Emission Scanning Electron Microscopy (FESEM) micrograph of iron oxide nanoparticles synthesized using Procedure 1. The resulting particles exhibit a non-uniform size distribution, ranging from 40 to 150 nm. These particles appear as thin flakes or disk-like shapes and display a tendency to aggregate more prominently. Figure 9 showcases the FESEM micrograph of iron oxide nanoparticles produced via Procedure 2. In this case, the particles display a mixed morphology, comprising both spherical and cubical shapes. The size range of these particles is observed to be between 45 and 90 nm. Figure 10 illustrates the FESEM micrograph of iron oxide nanoparticles synthesized by Procedure 3. The particles obtained through this method are smaller and exhibit a more uniform size distribution, ranging from 25 to 50 nm. Additionally, these particles are more spherical in shape compared to those shown in Figure 9.

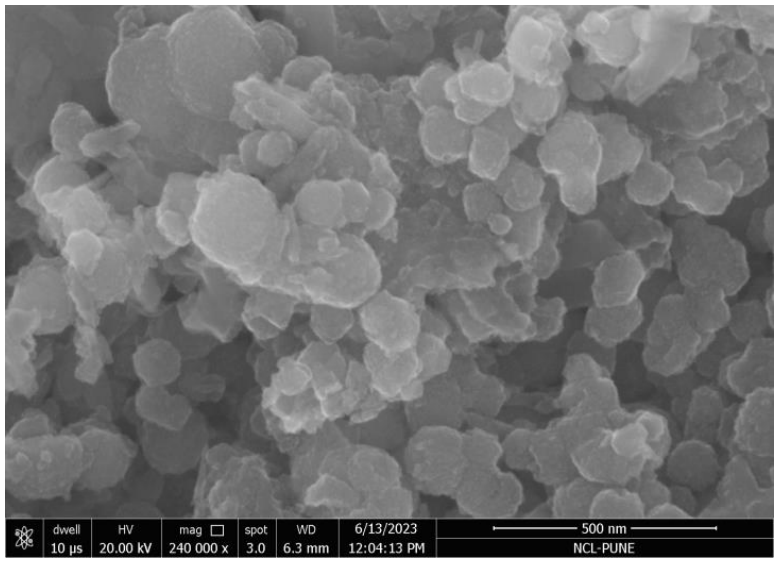

Fig. 8. FESEM micrograph of iron oxide synthesized without the use of stirring or ultrasonication.

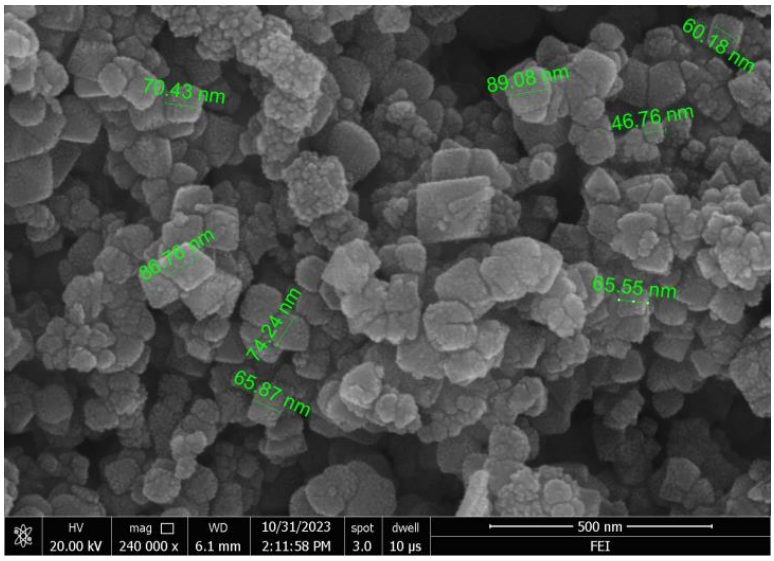

Fig. 9. FESEM micrograph of iron oxide synthesized with the use of stirring

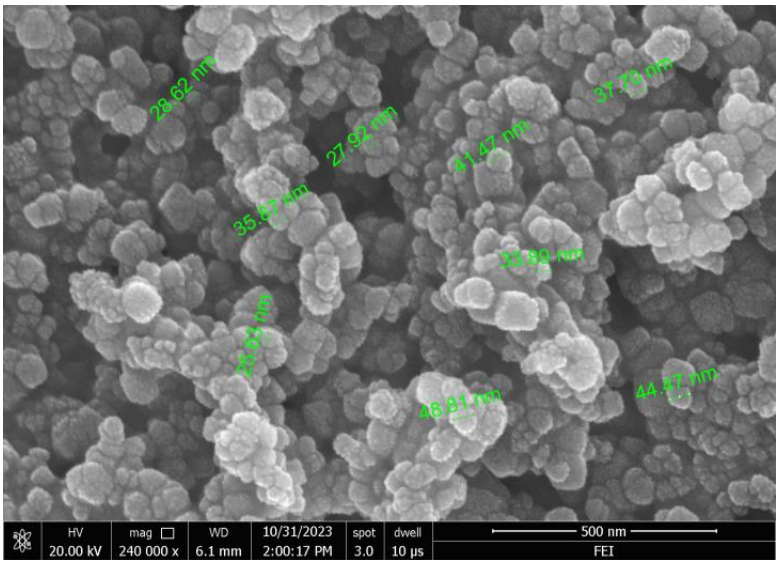

Fig. 10. FESEM micrograph of iron oxide synthesized in bath sonicator.

3.2. EDS analysis

Energy Dispersive Spectroscopy (EDS) is a powerful analytical technique used to determine the elemental composition of samples quantitatively. In this study, EDS was employed to analyse the iron oxide nanoparticles, and the results are presented in Figures 11, 12, and 13. The EDS spectra from these figures reveal distinct peaks corresponding to iron (Fe) and oxygen (O), confirming the formation of pure iron oxide nanoparticles. The presence and intensity of these peaks provide information about the relative amounts of each element in the sample. Specifically, the peaks in the EDS spectra indicate that the samples contain significant amounts of iron and oxygen, with minimal or no impurities. This suggests successful synthesis of high-purity iron oxide nanoparticles, which is crucial for their performance in various applications. Furthermore, Table 2 summarizes the quantitative composition of the iron oxide nanoparticles derived from the EDS analysis. This table provides detailed percentages of iron and oxygen present in the samples, offering a clear understanding of the sample's elemental makeup. The combination of EDS analysis and the summarized data in Table 2 provides a comprehensive view of the elemental composition of the synthesized nanoparticles, helping to validate the synthesis process and ensuring the desired chemical purity.

Table 2: The iron oxide nanoparticle composition obtained from EDS analysis

Sample Description	Wt %		At %	
Elements	Fe	O	Fe	O
Procedure 1	62.88	37.12	32.68	67.32
Procedure 2	61.14	38.86	31.07	68.93
Procedure 3	63.85	36.15	33.60	66.40

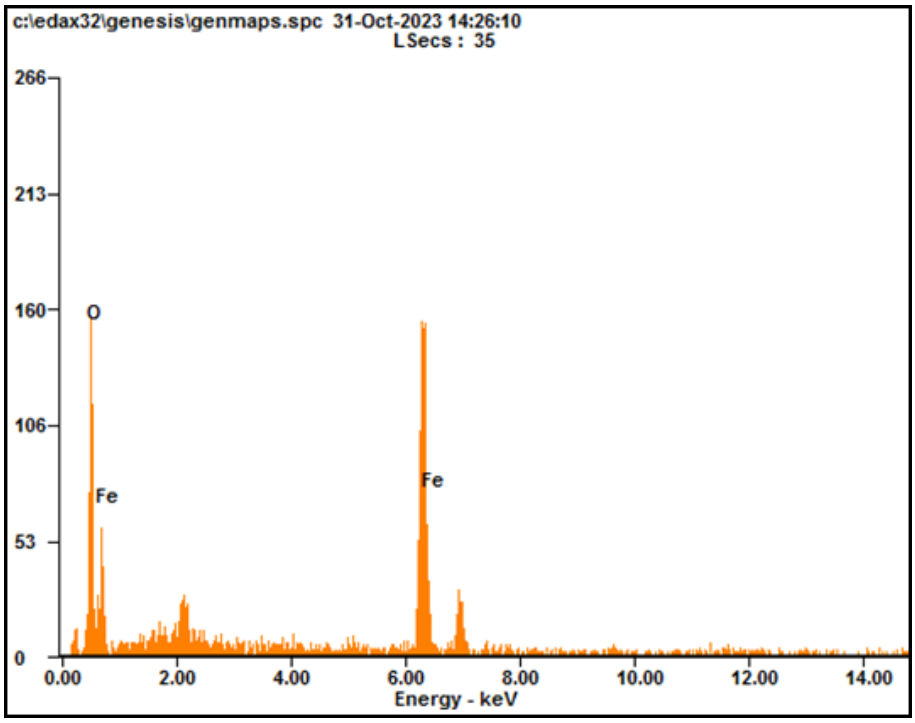

Fig. 11. EDS analysis of iron oxide nanoparticles synthesized without stirring or sonication.

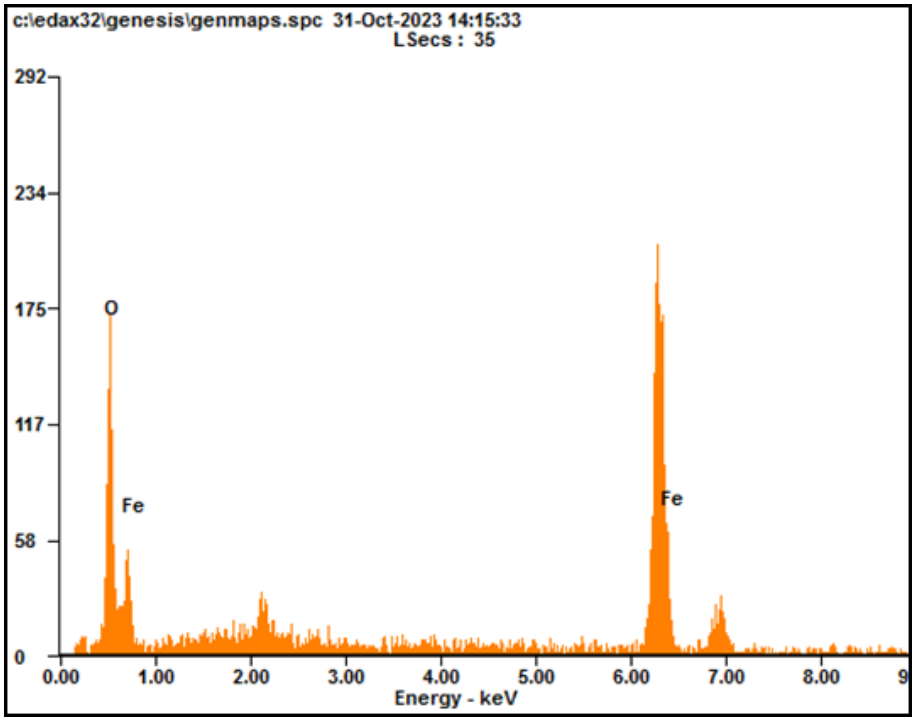

Fig. 12. EDS analysis of iron oxide nanoparticles synthesized with stirring.

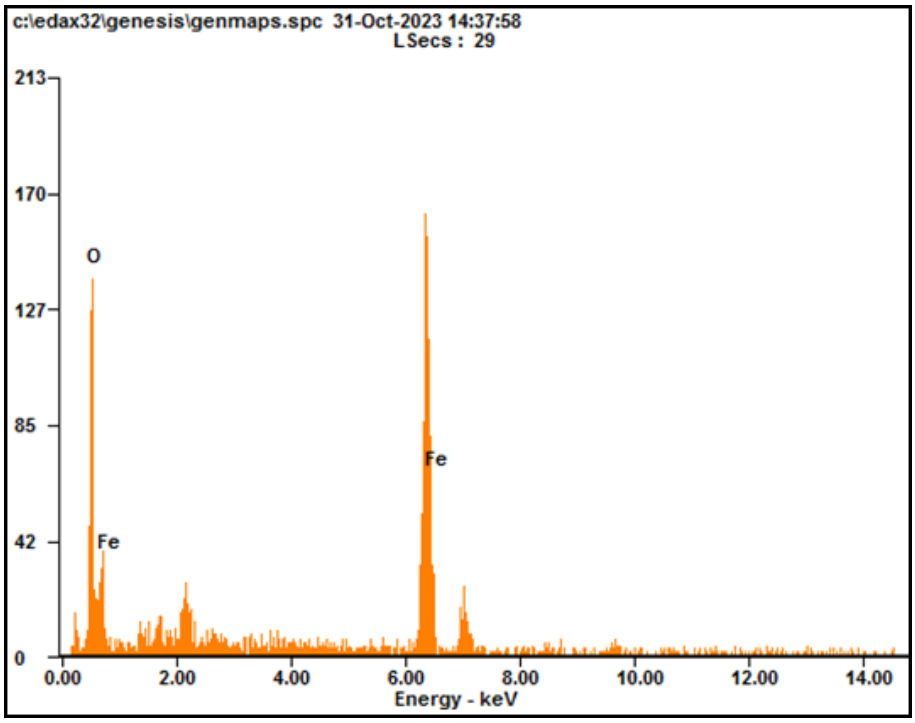

Fig. 13. EDS analysis of iron oxide nanoparticles synthesized in bath sonicator.

3.3. FTIR analysis

Figure 14 presents the Fourier Transform Infrared (FTIR) spectrum, which was used to analyse the presence of functional groups in all the samples. This technique provides insights into the chemical bonds and molecular structures of the synthesized iron oxide nanoparticles. In the spectrum, characteristic peaks corresponding to Fe-O stretching vibrations were observed within the ranges of 465 cm^{-1} and 551 cm^{-1}. These peaks confirm the formation of iron oxide, as these values are indicative of the Fe-O bond present in the nanoparticle structure. Additionally, the iron oxide nanoparticles exhibited a smaller peak at 1625 cm^{-1}. This peak is attributed to asymmetric COO- (carboxylate) stretching vibrations, suggesting that some surface functional groups or adsorbed species are present on the nanoparticles. FTIR spectroscopy is a valuable tool for identifying and confirming the presence of specific functional groups within a sample. The information obtained from these spectra is crucial for understanding the chemical composition and potential surface modifications of the iron oxide nanoparticles, which can influence their properties and applications in various fields.

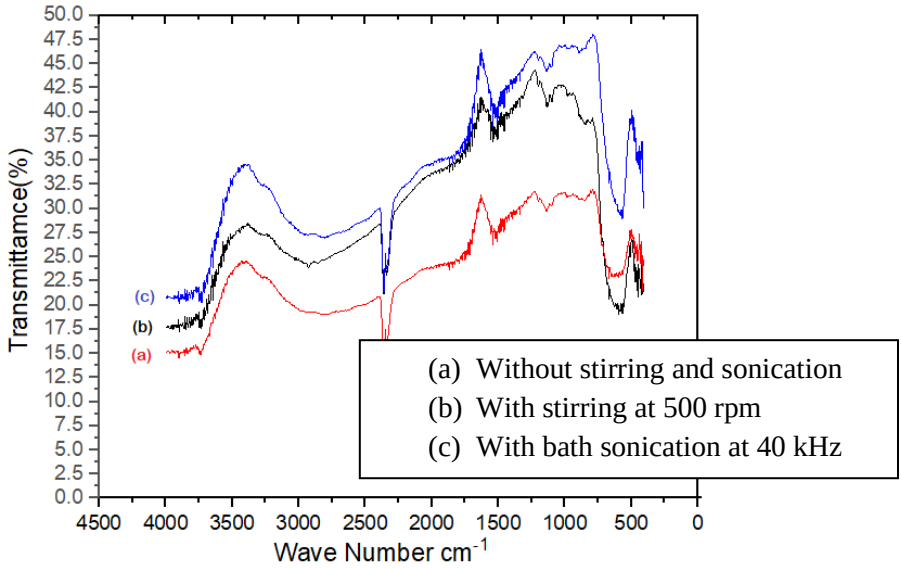

Fig. 14. FTIR spectrum of synthesized iron oxide nanoparticles

4. Conclusion:

The analysis of the results reveals that the initial mixing of the precursor and precipitant significantly impacts the properties of the iron oxide nanoparticles. This observation aligns with findings reported by various researchers in their studies. The co-precipitation reaction, when carried out using sonication, appears to be particularly promising due to the phenomenon of cavitation. Cavitation occurs when ultrasonic waves create microscopic bubbles in the liquid medium. These bubbles collapse rapidly, generating localized areas of high temperature and pressure. This effect acts as a source of energy that enhances local mixing, leading to a higher rate of nucleation and oxidation of the nanoparticles. Moreover, cavitation helps in reducing the aggregation of particles at later stages of the synthesis process. In contrast, mechanical stirring does not create the same conditions as sonication. As a result, it may not achieve the same level of local mixing and energy input, which are crucial for the nucleation and growth processes. Consequently, mechanical stirring often necessitates the use of stabilizers, surfactants, and additives to control particle size and prevent aggregation. However, these additional components can pose challenges during post-processing and may affect the final application of the nanoparticles.

In summary, the choice of mixing method at the initial stage plays a critical role in determining the size, morphology, and overall quality of the iron oxide nanoparticles. Sonication, with its cavitation-induced effects, offers a more efficient and effective approach compared to traditional mechanical stirring.

Declaration of Competing Interest:

The authors declare that they have no known competing financial interest or personal relationships that could appeared to influence the work report in this paper.

Acknowledgement:

Mr. Sunil M Badgujar, wish to acknowledge University Institute of Chemical Technology, Kavayitri Bahinabai Chaudhari North Maharashtra University Jalgaon, Maharashtra for allowing me to conduct the research work and utilize the laboratory infrastructure.

References

[1] D. Shi, Z. Guo, N. Bedford, Basic Properties of Nanomaterials, in: Nanomaterials and Devices, Elsevier, 2015: pp. 1–23. https://doi.org/10.1016/B978-1-4557-7754-9.00001-9.

[2] M.M. Can, M. Coşkun, T. Fırat, A comparative study of nanosized iron oxide particles; magnetite (Fe3O4), maghemite (γ-Fe2O3) and hematite (α-Fe2O3), using ferromagnetic resonance, Journal of Alloys and Compounds 542 (2012) 241–247. https://doi.org/10.1016/j.jallcom.2012.07.091.

[3] M. Mohapatra, S. Anand, Synthesis and applications of nano-structured iron oxides/hydroxides – a review, International Journal of Engineering, Science and Technology Vol. 2 (2010) 127–146. https://doi.org/10.4314/ijest.v2i8.63846.

[4] A. Ali, H. Zafar, M. Zia, I. Ul Haq, A.R. Phull, J.S. Ali, A. Hussain, Synthesis, characterization, applications, and challenges of iron oxide nanoparticles, NSA Volume 9 (2016) 49–67. https://doi.org/10.2147/NSA.S99986.

[5] W.S. Peternele, V. Monge Fuentes, M.L. Fascineli, J. Rodrigues Da Silva, R.C. Silva, C.M. Lucci, R. Bentes De Azevedo, Experimental Investigation of the Coprecipitation Method: An Approach to Obtain Magnetite and Maghemite Nanoparticles with Improved Properties, Journal of Nanomaterials 2014 (2014) 1–10. https://doi.org/10.1155/2014/682985.

[6] A.V. Rane, K. Kanny, V.K. Abitha, S. Thomas, Methods for Synthesis of Nanoparticles and Fabrication of Nanocomposites, in: Synthesis of Inorganic Nanomaterials, Elsevier, 2018: pp. 121–139. https://doi.org/10.1016/B978-0-08-101975-7.00005-1.

[7] F. Gilbert, P. Refait, F. Lévêque, C. Remazeilles, E. Conforto, Synthesis of goethite from Fe(OH)2 precipitates: Influence of Fe(II) concentration and stirring speed, Journal of Physics and Chemistry of Solids 69 (2008) 2124–2130. https://doi.org/10.1016/j.jpcs.2008.03.010.

[8] M.O. Besenhard, A.P. LaGrow, A. Hodzic, M. Kriechbaum, L. Panariello, G. Bais, K. Loizou, S. Damilos, M. Margarida Cruz, N.T.K. Thanh, A. Gavriilidis, Co-precipitation synthesis of stable iron oxide nanoparticles with NaOH: New insights and continuous production via flow chemistry, Chemical Engineering Journal 399 (2020) 125740. https://doi.org/10.1016/j.cej.2020.125740.

[9] A.M.S. Baptisttella, V.S. Madeira, C.M.B.D. Araujo, G. Rodrigues, J.S. Da Silva Neto, R.E.L.D. Abreu, The effect of operating conditions on iron oxides production–kinetics mechanism and final products characteristics, Mater. Res. Express 6 (2019) 045029. https://doi.org/10.1088/2053-1591/aafb24.

[10] M. Raz, F. Moztarzadeh, A.A. Hamedani, M. Ashuri, M. Tahriri, Controlled Synthesis, Characterization and Magnetic Properties of Magnetite (Fe3O4) Nanoparticles without Surfactant under N2 Gas at Room Temperature, KEM 493–494 (2011) 746–751. https://doi.org/10.4028/www.scientific.net/KEM.493-494.746.

[11] M. Loos, Processing of Polymer Matrix Composites Containing CNTs, in: Carbon Nanotube Reinforced Composites, Elsevier, 2015: pp. 171–188. https://doi.org/10.1016/B978-1-4557-3195-4.00006-0.

[12] P.R. Gogate, Cavitational reactors for process intensification of chemical processing applications: A critical review, Chemical Engineering and Processing: Process Intensification 47 (2008) 515–527. https://doi.org/10.1016/j.cep.2007.09.014.

[13] J.-H. Lee, S.U.S. Choi, S.P. Jang, S.Y. Lee, Production of aqueous spherical gold nanoparticles

using conventional ultrasonic bath, Nanoscale Res Lett 7 (2012) 420. https://doi.org/10.1186/1556-276X-7-420.

[14] G. Yang, W. Lin, H. Lai, J. Tong, J. Lei, M. Yuan, Y. Zhang, C. Cui, Understanding the relationship between particle size and ultrasonic treatment during the synthesis of metal nanoparticles, Ultrasonics Sonochemistry 73 (2021) 105497. https://doi.org/10.1016/j.ultsonch.2021.105497.

[15] S. Allahyari, M. Haghighi, A. Ebadi, S. Hosseinzadeh, Ultrasound assisted co-precipitation of nanostructured CuO–ZnO–Al2O3 over HZSM-5: Effect of precursor and irradiation power on nanocatalyst properties and catalytic performance for direct syngas to DME, Ultrasonics Sonochemistry 21 (2014) 663–673. https://doi.org/10.1016/j.ultsonch.2013.09.014.

[16] M.M. Ba-Abbad, A. Benamour, D. Ewis, A.W. Mohammad, E. Mahmoudi, Synthesis of Fe3O4 Nanoparticles with Different Shapes Through a Co-Precipitation Method and Their Application, JOM 74 (2022) 3531–3539. https://doi.org/10.1007/s11837-022-05380-3.